Quasinormal Modes of Modified Gravity (MOG) Black Holes

Luciano Manfredi,[1, a)] Jonas Mureika,[1, b)] and John Moffat[2, c)]

[1)]*Department of Physics, Loyola Marymount University, Los Angeles, CA 90045-2659, United States.*
[2)]*Perimeter Institute for Theoretical Physics, Waterloo, Ontario N2L 2Y5, Canada*

[a)]*Corresponding author: lmanfred@lion.lmu.edu*
[b)]*Electronic mail: jonas.mureika@lmu.edu*
[c)]*Electronic mail: jmoffat@perimeterinstitute.ca*

Abstract. Black holes play a fundamental role in modern physics. These possess characteristic resonant frequencies, called Quasinormal Modes (QNMs), which are important in our understanding of the dynamics of astrophysical black holes. Quasinormal modes are single frequency modes dominating the time evolution of perturbations of systems which are subject to damping, either by internal dissipation or by radiating away energy. Due to the damping, the frequency of a quasinormal mode must be complex, its imaginary part being inversely proportional to the typical damping time. In general relativity, damping occurs even without friction, since energy may be radiated away towards infinity by gravitational waves.

In this thesis, the quasinormal modes for gravitational and electromagnetic perturbations are calculated in a Scalar-Tensor-Vector (STVG) Modified Gravity (MOG) spacetime. This theory is based on an action principle and postulates the existence of a vector field, while elevating the three constants of the theory to scalar fields. In the weak-field approximation, STVG produces a Yukawa-like modification of the gravitational force due to a point source. STVG has been used successfully to explain galaxy rotation curves, the mass profiles of galaxy clusters, gravitational lensing in the Bullet Cluster, and cosmological observations without the need for dark matter.

It is found that for the increasing model parameter α, both the real and imaginary parts of the QNMs decrease compared to those for a Schwarzschild black hole. On the other hand, when taking into account the $1/(1+\alpha)$ mass re-scaling factor present in MOG, $\text{Im}(\omega)$ matches almost identically that of GR, while $\text{Re}(\omega)$ is higher. These results can be identified in the ringdown phase of massive compact object mergers, and are thus timely in light of the recent gravitational wave detections by LIGO.

INTRODUCTION

We are at the dawn of the era of gravitational wave astronomy. The five binary black hole merger signals observed by LIGO since September 2015 – GW150914 [1], GW-151226 [2], GW-170104 [3], GW-170608 [4] and GW170814 [5] – not only serve as concrete evidence of the existence of black holes, but allow us to explore classical (and potentially quantum) gravitational physics in a new fashion. A binary neutron star merger has also been observed (GW170817, [6]), giving more data for non-black compact objects. Gravitational waves also present a novel test of the underlying theory of gravitation, since their characteristics depend uniquely on the background spacetime structure. Such data can thus be a testbed for general relativity (GR) [7], as well as all alternate theories of gravitation [8, 9, 10, 11].

GW Event	Energy Radiated ($c^2 M_\odot$)	Chirp Mass ($M_\odot$)	Primary		Secondary		Remnant		
			Type	Mass ($M_\odot$)	Type	Mass ($M_\odot$)	Type	Mass ($M_\odot$)	Spin
GW150914	$3.0^{+0.5}_{-0.5}$	$28.2^{+1.8}_{-1.7}$	BH	$35.4^{+5.0}_{-3.4}$	BH	$29.8^{+3.3}_{-4.3}$	BH	$62.2^{+3.7}_{-3.4}$	$0.68^{+0.05}_{-0.06}$
GW151226	$1.0^{+0.1}_{-0.2}$	$8.9^{+0.3}_{-0.3}$	BH	$14.2^{+8.3}_{-3.7}$	BH	$7.5^{+2.3}_{-2.3}$	BH	$20.8^{+6.1}_{-1.7}$	$0.74^{+0.06}_{-0.06}$
GW170104	$2.0^{+0.6}_{-0.7}$	$21.1^{+2.4}_{-2.7}$	BH	$31.2^{+8.4}_{-6.0}$	BH	$19.4^{+5.3}_{-5.9}$	BH	$48.7^{+5.7}_{-4.6}$	$0.64^{+0.09}_{-0.20}$
GW170608	$0.85^{+0.07}_{-0.17}$	$7.9^{+0.2}_{-0.2}$	BH	12^{+7}_{-2}	BH	7^{+2}_{-2}	BH	$18.0^{+4.8}_{-0.9}$	$0.69^{+0.04}_{-0.05}$
GW170814	$2.7^{+0.4}_{-0.3}$	$24.1^{+1.4}_{-1.1}$	BH	$30.5^{+5.7}_{-3.0}$	BH	$25.3^{+2.8}_{-4.2}$	BH	$53.2^{+3.2}_{-2.5}$	$0.70^{+0.07}_{-0.05}$
GW170817	> 0.025	$1.188^{+0.004}_{-0.002}$	NS	1.36-1.60	NS	1.17 - 1.36	BH	$<2.74^{+0.04}_{-0.01}$	

TABLE I. Shows a list of the detected gravitational wave events from binary black hole (BH) and neutron star (NS) mergers [1] [2] [3] [4] [5] [6]. The chirp mass is similar to the geometric mean of the binary's masses, and is the binary parameter most relevant to the evolution of the inspiral gravitational waveform. $M_\odot$ stands for one solar mass.

Any object with mass that accelerates produces gravitational waves. However, gravitational waves made by us here on Earth are much too small to detect. In fact, it is not even remotely possible to build a machine that can spin an object fast enough to produce a detectable gravitational wave - even the world's strongest materials would fly apart at the rotation speeds such a machine would require.

Since we cannot generate detectable gravitational waves on Earth, the only way to study them is to look to the places in the Universe where they are generated by nature. The Universe is filled with incredibly massive objects that undergo rapid accelerations (things like black holes, neutron stars, and stars at the ends of their lives). These produce four different sources of gravitational waves: Compact Binary Inspiral Gravitational Waves, Continuous Gravitational Waves, Stochastic Gravitational Waves, and Burst Gravitational Waves. So far, all gravitational wave detections came from the first source, and this will be the one of interest for this thesis.

A binary merger signal (Fig. 1) is marked by three phases: the inspiral, merger, and ringdown. The characteristics of each phase yield important information about the nature of the merging objects (size, mass, spin, etc...). The inspiral phase is defined by the chirp frequency, and the associated waveform can be calculated for a given spacetime structure. The ringdown phase – in which the final black hole horizon "settles" down through damped oscillations –is in turn characterized by quasinormal mode vibrations (QNMs) [12]. The QNM distribution can be obtained from the ringdown phase of the merger, and can provide important insight into the process.
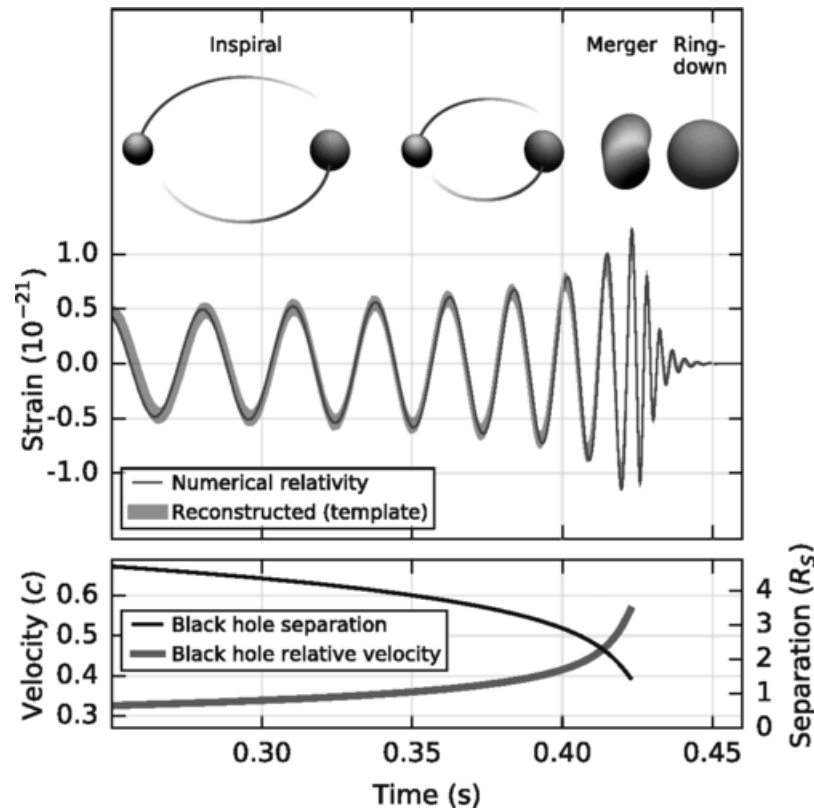
FIGURE 1. Illustration obtained from [1]. Top: Estimated gravitational-wave strain amplitude from GW150914 projected onto H1. The inset images show numerical relativity models of the black hole horizons as the black holes coalesce. Bottom: The Keplerian effective black hole separation in units of Schwarzschild radii ($R_S = 2GM/c^2$) and the effective relative velocity given by the post-Newtonian parameter $v/c = (GM\pi f/c^3)^{1/3}$, where f is the gravitational-wave frequency calculated with numerical relativity and M is the total mass.

It is likely that QNMs can be deciphered from such experimental data either in LIGO [14, 15, 16], or eventually in LISA [17]. Identification of model-dependent characteristics is thus of timely importance, including generic spacetime dependence, but also aspects such as the onset time for QNMs in mergers [19], and higher-order modes [18]. It has recently been pointed out that such data can also be useful in differentiating the type of compact objects that have merged [47].

In this thesis, we calculate quasinormal mode frequencies for static black holes in a Scalar-Tensor-Vector Gravity (STVG) gravity theory [21, 22, 23, 24, 25] using the Asymptotic Iteration Method (AIM) [20, 38]. We begin by reviewing the essentials of MOG, QNMs, and the AIM, after which we present the $\ell = 2, 3, 4$ frequencies of gravitational and $\ell = 1, 2, 3$ electromagnetic perturbations. The QNMs reduce to the standard values in the limit of general relativity. Lastly, we discuss the distinctions between MOG QNMs and GR QNMs, and consider the experimental detection of QNMs in either LIGO or LISA data, and the possibility of distinguihing GR from MOG QNMs.

SCALAR-TENSOR-VECTOR MODIFIED GRAVITY (MOG)

General Relativity Field Equations

In GR, gravity is formulated as a geometric interpretation, and as such, we must discard the classical Newtonian view of gravity. Instead, we can think of an object in a gravitational field as traveling along a geodesic in the semi-Riemannian manifold that represents 4-dimensional spacetime. Due to this geometric interpretation, geodesics are very important in describing motion due to gravity. A geodesic is commonly defined as the shortest distance between two points. One way to describe geodesics is by a concept called parallel transport. In this description, a path is considered a geodesic if it parallel transports its own tangent vectors at all points on the path. The act of parallel transporting a tangent vector relies specifically on how the curvature changes from point to point. As such, there is a natural way in which we can define a geodesic based on the intrinsic properties of that curvature. Mathematically, we denote this as

$$\frac{d^2 x^\lambda}{d\rho^2} + \Gamma^\lambda_{\mu\nu} \frac{dx^\mu}{d\rho} \frac{dx^\nu}{d\rho} = 0 \tag{1}$$

which is called the geodesic equation.

In the above, $\Gamma^\lambda_{\mu\nu}$ is a Christoffel symbol and is defined by

$$\Gamma^\lambda_{\mu\nu} = \frac{1}{2} g^{\lambda\beta} \left(\frac{\partial g_{\mu\beta}}{\partial x^\nu} + \frac{\partial g_{\nu\beta}}{\partial x^\mu} - \frac{\partial g_{\mu\nu}}{\partial x^\beta} \right) \tag{2}$$

where $g_{\mu\nu}$ is a component of the metric tensor, and in 4-D spacetime, λ, μ, and ν can be 0, 1, 2, or 3.

We now know that spacetime tells matter how to move, and matter tells spacetime how to curve. However, we have not yet described in what way matter, and specifically mass, influences the curvature of spacetime. This relation will be described by Einstein's field equations, which can be derived through the principle of least action.

Suppose that the full action of the theory is given by the Einstein-Hilbert term plus a term $\mathscr{L}_M$ describing any matter fields appearing in the theory:

$$S = \int \left[\frac{1}{2\kappa} R + \mathscr{L}_M \right] \sqrt{-g}\, \mathrm{d}^4 x \tag{3}$$

where $g = \det(g_{\mu\nu})$ is the determinant of the metric tensor matrix, R is the Ricci scalar, and $\kappa = 8\pi G_N c^{-4}$ is Einstein's constant (G_N is the gravitational constant and c is the speed of light in vacuum).

The action principle then tells us that the variation of this action with respect to the inverse metric is zero, yielding

$$
\begin{aligned}
0 &= \delta S \\
&= \int \left[\frac{1}{2\kappa} \frac{\delta(\sqrt{-g}R)}{\delta g^{\mu\nu}} + \frac{\delta(\sqrt{-g}\mathscr{L}_M)}{\delta g^{\mu\nu}} \right] \delta g^{\mu\nu} \mathrm{d}^4 x \\
&= \int \left[\frac{1}{2\kappa} \left(\frac{\delta R}{\delta g^{\mu\nu}} + \frac{R}{\sqrt{-g}} \frac{\delta \sqrt{-g}}{\delta g^{\mu\nu}} \right) + \frac{1}{\sqrt{-g}} \frac{\delta(\sqrt{-g}\mathscr{L}_M)}{\delta g^{\mu\nu}} \right] \delta g^{\mu\nu} \sqrt{-g}\, \mathrm{d}^4 x.
\end{aligned}
\tag{4}
$$

Since this equation should hold for any variation $\delta g^{\mu\nu} \delta g^{\mu\nu}$, it implies that

$$\frac{\delta R}{\delta g^{\mu\nu}} + \frac{R}{\sqrt{-g}} \frac{\delta \sqrt{-g}}{\delta g^{\mu\nu}} = -2\kappa \frac{1}{\sqrt{-g}} \frac{\delta(\sqrt{-g}\mathscr{L}_M)}{\delta g^{\mu\nu}}, \tag{5}$$

is the equation of motion for the metric field. The right hand side of this equation is (by definition) proportional to the stress-energy tensor,

$$T_{\mu\nu} := \frac{-2}{\sqrt{-g}} \frac{\delta(\sqrt{-g}\mathscr{L}_{\mathrm{M}})}{\delta g^{\mu\nu}} = -2\frac{\delta\mathscr{L}_{\mathrm{M}}}{\delta g^{\mu\nu}} + g_{\mu\nu}\mathscr{L}_{\mathrm{M}}. \tag{6}$$

To calculate the left hand side of the equation we need the variations of the Ricci scalar R and the determinant of the metric. These can be obtained by standard text book calculations:

$$\frac{\delta R}{\delta g^{\mu\nu}} = R_{\mu\nu} = \partial_\nu \Gamma_{\mu\sigma}{}^\sigma - \partial_\sigma \Gamma_{\mu\nu}{}^\sigma + \Gamma^\alpha_{\mu\sigma}\Gamma^\sigma_{\alpha\nu} - \Gamma^\alpha_{\mu\nu}\Gamma^\sigma_{\alpha\sigma} \tag{7}$$

$$\frac{1}{\sqrt{-g}} \frac{\delta\sqrt{-g}}{\delta g^{\mu\nu}} = -\frac{1}{2}g_{\mu\nu}. \tag{8}$$

Now that we have all the necessary variations at our disposal, we can insert them into the equation of motion for the metric field to obtain,

$$R_{\mu\nu} - \frac{1}{2}g_{\mu\nu}R = \frac{8\pi G_N}{c^4}T_{\mu\nu}, \tag{9}$$

which is Einstein's field equation and

$$\kappa = \frac{8\pi G_N}{c^4} \tag{10}$$

has been chosen such that the non-relativistic limit yields the usual form of Newton's gravity law, where G_N is the gravitational constant.

General Relativity Black Holes

The history behind the genesis of the concept of black holes began very shortly after Einstein published his first articles on GR in November 1915. Indeed, Schwarzschild, then serving in the German artillery on the Russian front, found the following solution to Einstein's equations in vacuum ($G_N = c = 1$):

$$ds^2 = \left(1 - \frac{2M}{r}\right)dt^2 - \left(1 - \frac{2M}{r}\right)^{-1}dr^2 - r^2 d\theta^2 - r^2 \sin^2\theta d\phi^2. \tag{11}$$

This solution would thereafter bear his name. This is an immediate confirmation that one should be wary of Newtonian intuition while dealing with GR: even without matter, Einstein's equations admit non-trivial solutions, whose properties are quite different from Minkowski spacetime:

$$ds^2 = dt^2 - dr^2 - r^2 d\theta^2 - r^2 \sin^2\theta \, d\phi^2 \tag{12}$$

here in spherical coordinates. Schwarzschild died shortly after that, in May 1916, from a disease contracted in the trenches, but not before succeeding in matching this solution (11) with the interior of a star of constant energy density and pressure.

Coming back to the solution (11), several properties immediately attract our attention. The metric coefficients are ill-behaved both at $r = 0$ and at $r = 2M$, but scalar invariants, like for example the Kretschmann invariant, diverge only at $r = 0$:

$$K \equiv R_{\lambda\mu\nu\rho}R^{\lambda\mu\nu\rho} = \frac{48M^2}{r^6} \tag{13}$$

which signals the presence of a true curvature singularity.

The nature of the so-called "Schwarzschild singularity" at $r_S = 2M$ was however much more troubling. Were one to cross it somehow, time and space would be reversed. In pretty much the same way as an observer outside the Schwarzschild radius could follow a time-like wordline while sitting in the same point in space, an equivalent observer inside would see space flow by irrevocably while time could be kept frozen! Namely, the metric signature changes from $(+,-,-,-)$ to $(-,+,-,-)$. Thus, having exchanged the role of time and space inside the Schwarzschild radius, space (which is now time) can but flow, and so one falls inexorably in the singularity: the singularity is the endpoint, past or future, of all time-like trajectories.

This provides a global definition for black holes, instead of depending upon a local system of coordinates. A spacetime will contain a black hole if there is a region of spacetime causally disconnected from future infinity. The horizon of the black hole is the boundary of such a region.

MOG Field Equations

Scalar-Tensor-Vecor STVG MOdified Gravity (MOG) [21] has been studied as an alternative to GR without detectable dark matter in the present universe and fits to galaxy rotation curves and galaxy clusters have been obtained [26, 27, 28]. The theory has also been applied to cosmology explaining early universe structure growth and the Cosmic Microwave Background (CMB) data [29, 30, 31].

We begin with the Einstein-Hilbert Lagrangian:

$$\mathscr{L}_G = -\frac{1}{16\pi G}R\sqrt{-g}, \tag{14}$$

where R is the trace of the Ricci tensor, G_N is the gravitational constant and g is the determinant of the metric tensor $g_{\mu\nu}$.

We introduce the Maxwell-Proca Lagrangian for the STVG vector field ϕ_μ:

$$\mathscr{L}_\phi = -\frac{1}{4\pi}\omega\left[\frac{1}{4}B^{\mu\nu}B_{\mu\nu} - \frac{1}{2}\mu^2\phi_\mu\phi^\mu + V_\phi(\phi)\right]\sqrt{-g}, \tag{15}$$

where $B_{\mu\nu} = \partial_\mu\phi_\nu - \partial_\nu\phi_\mu$, μ is the vector field mass, ω characterizes the strength of the coupling between the fifth force and matter, and V_ϕ is a self-interaction potential.

The three constants of the theory, G, μ and ω, are promoted to scalar fields by introducing associated kinetic and potential terms in the Lagrangian density:

$$\mathscr{L}_S = -\frac{1}{G}\left[\frac{1}{2}g^{\mu\nu}\left(\frac{\nabla_\mu G\nabla_\nu G}{G^2} + \frac{\nabla_\mu\mu\nabla_\nu\mu}{\mu^2} - \nabla_\mu\omega\nabla_\nu\omega\right) + \frac{V_G(G)}{G^2} + \frac{V_\mu(\mu)}{\mu^2} + V_\omega(\omega)\right]\sqrt{-g}, \tag{16}$$

where ∇_μ denotes covariant differentiation with respect to the metric $g_{\mu\nu}$, while V_G, V_μ, and V_ω are the self-interaction potentials associated with the scalar fields.

The STVG action integral takes the form

$$S = (\oint_G + \mathscr{L}_\phi + \mathscr{L}_S + \mathscr{L}_M)\, d^4x. \tag{17}$$

Using the variational principle on the action integral, we obtain the STVG field equations given by ($c = 1$):

$$G_{\mu\nu} - \Lambda g_{\mu\nu} + Q_{\mu\nu} = -8\pi G T_{\mu\nu}, \tag{18}$$

$$\frac{1}{\sqrt{-g}}\partial_\nu(\sqrt{-g}B^{\mu\nu}) + \mu^2\phi^\mu = -J^\mu, \tag{19}$$

$$\partial_\sigma B_{\mu\nu} + \partial_\mu B_{\nu\sigma} + \partial_\nu B_{\sigma\mu} = 0, \tag{20}$$

$$\Box G = K(x), \tag{21}$$

$$\Box\mu = L(x). \tag{22}$$

We have

$$Q_{\mu\nu} = \frac{2}{G^2}(\partial^\alpha G\partial_\alpha G g_{\mu\nu} - \partial_\mu G\partial_\nu G) - \frac{1}{G}(\Box G g_{\mu\nu} - \nabla_\mu\partial_\nu G). \tag{23}$$

Moreover,

$$K(x) = \frac{3}{G}\left(\frac{1}{2}\partial^\alpha G\partial_\alpha G - V(G)\right) - \frac{3}{G}\partial^\alpha G\partial_\alpha G + \frac{G}{\mu^2}\left(\frac{1}{2}\partial^\alpha\mu\partial_\alpha\mu - V(\mu)\right) + \frac{3G^2}{16\pi}\Box\left(\frac{1}{G}\right), \tag{24}$$

and

$$L(x) = -\left(\frac{1}{G}\partial^\alpha G\partial_\alpha\mu + \frac{2}{\mu}\partial^\alpha\mu\partial_\alpha\mu - \mu^2 G\frac{\partial V(\phi_\mu))}{\partial\mu}\right), \tag{25}$$

where $V(\phi_\mu) = (1/2)\mu^2\phi^\mu\phi_\mu$. Moreover, $G_{\mu\nu}$ is the Einstein tensor $G_{\mu\nu} = R_{\mu\nu} - \frac{1}{2}g_{\mu\nu}R$, Λ is the cosmological constant, ∇_μ is the covariant derivative with respect to $\Gamma^\lambda_{\mu\nu}$, $\Box = \nabla^\mu\nabla_\mu$, $T = g^{\mu\nu}T_{\mu\nu}$, G and μ are scalar fields and $V(G)$ and $V(\mu)$ are potentials. The Ricci curvature tensor is defined just like in GR (7), but the total energy-momentum tensor is

$$T_{\mu\nu} = T^M_{\mu\nu} + T^\phi_{\mu\nu} + T^G_{\mu\nu} + T^\mu_{\mu\nu}, \tag{26}$$

where $T^M_{\mu\nu}$ is the energy-momentum tensor for ordinary matter, and

$$T^{(\phi)}_{\mu\nu} = -\frac{1}{4\pi}\left[B^\alpha_\mu B_{\nu\alpha} - g_{\mu\nu}\left(\frac{1}{4}B^{\rho\alpha}B_{\rho\alpha} + V(\phi_\mu)\right) + 2\frac{\partial V(\phi_\mu)}{\partial g^{\mu\nu}}\right], \tag{27}$$

$$T^{(G)}_{\mu\nu} = -\frac{1}{4\pi G^3}\left(\partial_\mu G\partial_\nu G - \frac{1}{2}g_{\mu\nu}\partial_\alpha G\partial^\alpha G\right), \tag{28}$$

$$T^{(\mu)}_{\mu\nu} = -\frac{1}{4\pi G\mu^2}\left(\partial_\mu\mu\partial_\nu\mu - \frac{1}{2}g_{\mu\nu}\partial_\alpha\mu\partial^\alpha\mu\right). \tag{29}$$

The covariant current density J^μ for matter is defined by

$$J^\mu = \kappa T^{M\mu\nu}u_\nu, \tag{30}$$

where $\kappa = \sqrt{\alpha G_N}$, $\alpha = (G - G_N)/G_N$ is a dimensionless scalar field, G_N is Newton's constant, $u^\mu = dx^\mu/ds$ and s is the proper time along a particle trajectory. The perfect fluid energy-momentum tensor for matter is given by

$$T^{M\mu\nu} = (\rho_M + p_M)u^\mu u^\nu - p_M g^{\mu\nu}, \tag{31}$$

where ρ_M and p_M are the density and pressure of matter, respectively, and for the fluid u^μ is the comoving four-velocity. We get from (30) and (31) by using $u^\nu u_\nu = 1$:

$$J^\mu = \kappa\rho_M u^\mu. \tag{32}$$

The gravitational source charge is given by

$$Q_g = \int d^3x J^0(x). \tag{33}$$

MOG Black Holes

An exact generalized Schwarzschild-MOG solution of the STVG fields equations is obtained by requiring that $G = G_N(1 + \alpha) \sim$ constant and $Q_g = \sqrt{\alpha G_N} M \sim$ constant, and ignoring the small ϕ_μ field particle mass $m_\phi \sim 10^{-28}$ eV in the present universe. This mass is obtained from fitting STVG to the galaxy and cluster data [26], [27]. The field equations are given by

$$R_{\mu\nu} = -8\pi G T_{\mu\nu}^\phi, \tag{34}$$

$$\frac{1}{\sqrt{-g}} \partial_\nu (\sqrt{-g} B^{\mu\nu}) = 0, \tag{35}$$

$$\partial_\sigma B_{\mu\nu} + \partial_\mu B_{\nu\sigma} + \partial_\nu B_{\sigma\mu} = 0. \tag{36}$$

The energy-momentum tensor $T^{(\phi)}{}_\mu{}^\nu$ is

$$T^{(\phi)}{}_\mu{}^\nu = -\frac{1}{4\pi} \left(B_{\mu\alpha} B^{\nu\alpha} - \frac{1}{4} \delta_\mu{}^\nu B^{\alpha\beta} B_{\alpha\beta} \right). \tag{37}$$

The metric is given by

$$\begin{aligned} ds^2 = \left(1 - \frac{2G_N(1+\alpha)M}{r} + \frac{\alpha(1+\alpha)G_N^2 M^2}{r^2} \right) dt^2 \\ - \left(1 - \frac{2G_N(1+\alpha)M}{r} + \frac{\alpha(1+\alpha)G_N^2 M^2}{r^2} \right)^{-1} dr^2 - r^2 d\Omega^2. \end{aligned} \tag{38}$$

This has the form of the static, spherically symmetric point particle Reissner-Nordstrom solution for an electrically charged black hole, but now the charge $Q_g > 0$ is of gravitational origin. As in the case of astrophysical bodies, black holes are not expected to possess electric charge.

The MOG black hole possesses two horizons given by

$$r_\pm = G_N M \left[1 + \alpha \pm (1 + \alpha)^{1/2} \right]. \tag{39}$$

Note that we obtain the Schwarzschild black hole when $\alpha = 0$ giving $r_+ = r_s = 2G_N M$ as expected.

A generalized Kerr-MOG black hole solution has also been derived [23]. The metric is

$$ds^2 = \frac{\Delta}{\rho^2} (dt - a\sin^2\theta d\phi)^2 - \frac{\sin^2\theta}{\rho^2} [(r^2 + a^2)d\phi - a dt]^2 - \frac{\rho^2}{\Delta} dr^2 - \rho^2 d\theta^2, \tag{40}$$

where

$$\Delta = r^2 - 2GMr + a^2 + \alpha(1+\alpha)G_N^2 M^2, \quad \rho^2 = r^2 + a^2 \cos^2\theta. \tag{41}$$

The spacetime geometry is axially symmetric around the z axis. Horizons are determined by the roots of $\Delta = 0$:

$$r_\pm = G_N(1+\alpha)M \left[1 \pm \sqrt{1 - \frac{a^2}{G_N^2(1+\alpha)^2 M^2} - \frac{\alpha}{1+\alpha}} \right]. \tag{42}$$

An ergosphere horizon is determined by $g_{00} = 0$:

$$r_E = G_N(1+\alpha)M \left[1 + \sqrt{1 - \frac{a^2 \cos^2\theta}{G_N^2(1+\alpha)^2 M^2} - \frac{\alpha}{1+\alpha}} \right]. \tag{43}$$

The solution is fully determined by the Arnowitt-Deser-Misner (ADM) mass M and spin parameter a ($a = S/GM^2$ where S denotes the spin-angular momentum) measured by an asymptotically distant observer. When $a = 0$ the solution reduces to the Schwarzschild MOG black hole metric (38).

CALCULATING QUASINORMAL MODES

Overview

Investigations concerning the interaction of black holes with surrounding fields give us the possibility to learn about black hole physics. Some of this information can be obtained from Quasinormal Modes (QNMs), which are characteristic to the background black hole's space-time. QNMs present complex frequencies, whose real part gives the actual frequency while the imaginary part dictates the damping.

The QNM gravitational perturbations are considered to be the most important type of perturbations to be analyzed, since they can directly identify black holes and their gravitational radiation. In other words, gravitational QNMs serve as a unique fingerprint when searching for the existence of black holes. With the newly launched era of gravitational wave astronomy, triggered by the detection of a transient gravitational-wave signal determined to be the coalescence of two black holes back on September 14th, 2015, the understanding of QNMs grew in popularity, and even more for alternative theories of gravity like the one examined in this thesis.

Formally, QNMs are solutions to perturbed gravitational field equations subject to the two boundary conditions

$$\psi(x) \longrightarrow \begin{cases} e^{-i\omega x} & x \to -\infty \\ e^{i\omega x} & x \to \infty \end{cases} \tag{44}$$

where the positive and negative solutions correspond to ingoing and outgoing waves, respectively.

Calculation of these quantities often requires a numerically-intensive procedure, and furthermore the boundary conditions listed above are not satisfied in a wide range of cases. This leads one to identify the QNMs as the discrete values where the above holds true.

With the emergence of accessible large-scale computing over the last two decades, several new methods have emerged as viable avenues to obtaining QNMs. Among the most popular ones, there is the semi-analytic formalism employed by Ferrari and Mashoon *et al.* [32], the Continued Fraction Method (CFM) developed by Leaver [33], and the WKB approximation [34]. In recent years, the asymptotic iteration method (AIM) was shown to be more efficient in certain cases [37].

Asymptotic Iteration Method

The AIM we adopt to calculate QNMs is detailed in [20, 38], and will be the machinery of focus in this thesis. We reproduce the essential components of the method here.

We begin by defining a second-order differential equation of the form

$$\chi'' = \lambda_0(x)\chi' + s_0(x)\chi. \tag{45}$$

The functions $\lambda_0(x)$ and $s_0(x)$ are well defined and sufficiently smooth, which allows us to further differentiate the above to obtain

$$\chi''' = \lambda_1(x)\chi' + s_1(x)\chi. \tag{46}$$

Here, the new coefficients are: $\lambda_1(x) = \lambda_0' + s_0 + \lambda_0^2$ and $s_1(x) = s_0' + s_0\lambda_0$.

Proceeding from an iterative approach in the order of differentiation, one eventually arrives at the general expression

$$\chi^{(n+2)} = \lambda_n(x)\chi' + s_n(x)\chi, \tag{47}$$

where the coefficients satisfy the relations

$$\lambda_n(x) = \lambda_{n-1}' + s_{n-1} + \lambda_0\lambda_{n-1}, \quad s_n(x) = s_{n-1}' + s_0\lambda_{n-1}. \tag{48}$$

For *n* large enough, the AIM feature is manifested by requiring

$$\frac{s_n(x)}{\lambda_n(x)} = \frac{s_{n-1}(x)}{\lambda_{n-1}(x)} \equiv \beta(x). \tag{49}$$

The QNMs thus arise from a "quantization condition" marking an end to the algorithm [35],

$$\delta_n = s_n\lambda_{n-1} - s_{n-1}\lambda_n = 0. \tag{50}$$

Nevertheless, these recursion relations (48) are not numerically optimal to evaluate [36], since differentiation of the λ and s terms in previous steps needs to be taken repetitively. The parameters λ_n and s_n are Taylor-expanded about the point ξ,

$$\lambda_n(\xi) = \sum_{i=0}^{\infty} c_n^i (x - \xi)^i \tag{51}$$

$$s_n(\xi) = \sum_{i=0}^{\infty} d_n^i (x - \xi)^i, \tag{52}$$

with the values c_n^i and d_n^i representing the ith Taylor constants of $\lambda_n(\xi)$ and $s_n(\xi)$.

A new recursive expression is obtained after substituting the above values into (48),

$$c_n^i = (i+1)c_{n-1}^{i+1} + d_{n-1}^i + \Sigma_{k=0}^i c_0^k c_{n-1}^{i-k} \tag{53}$$

$$d_n^i = (i+1)d_{n-1}^{i+1} + \Sigma_{k=0}^i d_0^k c_{n-1}^{i-k}. \tag{54}$$

Now the quantization condition (50) is cast in the new form as:

$$d_n^0 c_{n-1}^0 - d_{n-1}^0 c_n^0 = 0, \tag{55}$$

which saves computational time [38].

Quasinormal Modes of Static MOG Black Holes

Rescaling $2M = 1$ in natural units $G_N = c = 1$ makes QNMs dependent on Q_g, ℓ, and n. The new metric function is:

$$f(r) = 1 - \frac{1+\alpha}{r} + \frac{\alpha(1+\alpha)}{4r^2}. \tag{56}$$

Outside the event horizon, STVG MOG perturbation equations are separable and produce the even- and odd-parity oscillations:

$$\left(\frac{d^2}{dx^2} - \rho^2 - V_i^{(\pm)}\right) Z_i^{(\pm)} = 0. \tag{57}$$

Even and odd modes are represented by $+$ and $-$ respectively [39] [40] [41]:

$$V_i^{(-)}(r) = \frac{\Delta}{r^5}\left(Ar - q_j + \frac{4Q_g^2}{r}\right) \tag{58}$$

$$V_i^{(+)}(r) = V_i^{(-)}(r) + 2q_j \frac{d}{dx}\left(\frac{\Delta}{r^2[(\ell-1)(\ell+2)r + q_j]}\right) \tag{59}$$

for $i = j = (1,2)(i \neq j)$ and

$$\frac{dr}{dx} = \frac{\Delta}{r^2}, \tag{60}$$

$$\Delta = (r - r_+)(r - r_-) = \tfrac{1}{4}[4r^2 - 4r(1+\alpha) + \alpha(1+\alpha)], \tag{61}$$

$$A = \ell(\ell+1), \tag{62}$$

$$q_1 = \tfrac{1}{2}\left[3 + \sqrt{9 + 16Q_g^2(\ell-1)(\ell+2)}\right], \tag{63}$$

$$q_2 = \tfrac{1}{2}\left[3 - \sqrt{9 + 16Q_g^2(\ell-1)(\ell+2)}\right], \tag{64}$$

$$\rho = -i\omega. \tag{65}$$

Above ω denotes frequency, ℓ the rotational parameter and r_- and r_+ correspond to the two event horizon radii. In the $\alpha = 0$ limit, $r_+ = 1$ and $r_- = 0$ as expected.

Because the effective potential $V_i^{(-)}$ is easier to deal with than $V_i^{(+)}$, QNMs are calculated for the odd-parity modes. The isospectrality between the QNMs of the odd and even perturbations was numerically determined to hold. Indeed, the two potentials $V_i^{(-)}$ and $V_i^{(+)}$ share the same spectra of QNMs.

The tortoise coordinate is

$$x = \int \frac{r^2}{\Delta} = r + \frac{r_+^2}{r_+ - r_-}\ln(r - r_+) - \frac{r_-^2}{r_+ - r_-}\ln(r - r_-), \tag{66}$$

and varies between $(-\infty, \infty)$ starting at the horizon off to infinity.

First, changing variables from $x \to r$ using (60):

$$\frac{d}{dx} = \frac{\Delta}{r^2}\frac{d}{dr} \tag{67}$$

and

$$\frac{d^2}{dx^2} = \left(\frac{\Delta}{r^2}\right)\left(\frac{(2r - \alpha)(1 + \alpha)}{2r^3}\right)\frac{d}{dr} + \left(\frac{\Delta}{r^2}\right)^2\frac{d^2}{dr^2}. \tag{68}$$

Substituting back in (57) yields

$$\left(\frac{\Delta}{r^2}\right)^2\frac{d^2}{dr^2}Z_i^{(-)} + \left(\frac{\Delta}{r^2}\right)\left(\frac{(2r - \alpha)(1 + \alpha)}{2r^3}\right)\frac{d}{dr}Z_i^{(-)} - \left[\rho^2 + V_i^{(-)}\right]Z_i^{(-)} = 0 \tag{69}$$

where $Z_i^{(-)}$ satisfies the boundary conditions:

$$Z_i^{(-)} \longrightarrow \begin{cases} e^{-i\omega x} & x \to -\infty \\ e^{i\omega x} & x \to \infty \end{cases} \tag{70}$$

The asymptotic behavior is introduced by imposing the previous condition to $Z_i^{(-)}$ [42], giving

$$Z_i^{(-)} = e^{-\rho r}r^{-1}(r - r_1)^{1-\rho - \frac{\rho r_+^2}{r_+ - r_-}}(r - r_+)^{\frac{\rho r_+^2}{r_+ - r_-}}\chi_{Z_i}(r). \tag{71}$$

Taking the r derivative of $Z_i^{(-)}$ once and twice leads to

$$Z_{i,r}^{(-)} \equiv \frac{d}{dr}Z_i^{(-)} = e^{-\rho r}r^{-1}(r - r_1)^{1-\rho - \frac{\rho r_+^2}{r_+ - r_-}}(r - r_+)^{\frac{\rho r_+^2}{r_+ - r_-}}\left(\chi_{Z_{i,r}} + \Gamma_Z\chi_{Z_i}\right) \tag{72}$$

and

$$Z_{i,rr}^{(-)} = e^{-\rho r}r^{-1}(r - r_1)^{1-\rho - \frac{\rho r_+^2}{r_+ - r_-}} \times (r - r_+)^{\frac{\rho r_+^2}{r_+ - r_-}}\left(\chi_{Z_{i,rr}} + 2\Gamma_Z\chi_{Z_{i,r}} + (\Gamma_Z^2 + \Gamma_{Z,r})\chi_{Z_i}\right) \tag{73}$$

where

$$\Gamma_Z = -\rho - \frac{1}{r} + \frac{(1 - \rho)(r_+ - r_-) - \rho r_+^2}{(r_+ - r_-)(r - r_-)} + \frac{\rho r_+^2}{(r_+ - r_-)(r - r_+)}. \tag{74}$$

Replacing (72) and (73) into Eqn. (69) gives

$$\left(\frac{\Delta}{r^2}\right)^2\chi_{Z_{i,rr}} + \left[2\Gamma_Z\left(\frac{\Delta}{r^2}\right)^2 + \left(\frac{\Delta}{r^2}\right)\left(\frac{(2r - \alpha)(1 + \alpha)}{2r^3}\right)\right]\chi_{Z_{i,r}} + $$
$$\left\{\left(\frac{\Delta}{r^2}\right)^2(\Gamma_Z^2 + \Gamma_{Z,r}) + \left(\frac{\Delta}{r^2}\right)\left(\frac{(2r - \alpha)(1 + \alpha)}{2r^3}\right)\Gamma_Z - \left[\rho^2 + V_i^{(-)}\right]\right\}\chi_{Z_i} = 0. \tag{75}$$

Following this step, a change of coordinate variables is performed such that $r \to \xi$ with $\xi = 1 - \frac{r_+}{r}$, which ranges between [0,1] for r between the horizon and infinity. Then

$$\frac{d}{dr} = \frac{(1 - \xi)^2}{r_+}\frac{d}{d\xi} \tag{76}$$

and

$$\frac{d^2}{dr^2} = \frac{(1-\xi)^4}{r_+^2}\frac{d^2}{d\xi^2} - 2\frac{(1-\xi)^3}{r_+^2}\frac{d}{d\xi}. \tag{77}$$

Plugging these back in and recasting the equation to perform the AIM yields

$$\chi_{Z_i,\xi\xi} = \lambda_{Z_i}(\xi)\chi_{Z_i,\xi} + s_{Z_i}(\xi)\chi_{Z_i}, \tag{78}$$

where

$$\lambda_{Z_i}(\xi) = \frac{\alpha(\alpha+1)+4\Delta}{2\Delta(1-\xi)} - \frac{r_+(\alpha+2\Gamma_Z\Delta+1)}{\Delta(\xi-1)^2}, \tag{79}$$

$$s_{Z_i}(\xi) = \frac{r_+^6\left(\rho^2+V_i^{(-)}\right)}{\Delta^2(\xi-1)^8} - \frac{\Gamma_Z r_+^2(1+\alpha+\Delta\Gamma_Z)}{\Delta(\xi-1)^4} - \frac{\alpha(\alpha+1)\Gamma_Z r_+}{2\Delta(\xi-1)^3} - \frac{r_+\Gamma_{Z,\xi}}{(\xi-1)^2} \tag{80}$$

$$\Gamma_Z = -\rho - \frac{1-\xi}{r_+} + \frac{\left[(1-\rho)(r_+-r_-)-\rho r_+^2\right](1-\xi)}{(r_+-r_-)\left[r_+-r_-(1-\xi)\right]} + \frac{\rho r_+(1-\xi)}{(r_+-r_-)\xi}, \tag{81}$$

$$V_i^{(-)} = \Delta\frac{(1-\xi)^5}{r_+^5}\left[\frac{Ar_+}{1-\xi} - q_j + \frac{4Q_g^2(1-\xi)}{r_+}\right], \tag{82}$$

$$\Delta = \frac{r_+\xi\left[r_+-r_-(1-\xi)\right]}{(1-\xi)^2} = \frac{(1+\alpha)\xi\left(2+2\sqrt{1+\alpha}+\alpha\xi\right)}{4(\xi-1)^2}, \tag{83}$$

$$r_\pm = \frac{1}{2}\left[1+\alpha\pm(1+\alpha)^{1/2}\right], \tag{84}$$

$$Q_g = \frac{\sqrt{\alpha}}{2}. \tag{85}$$

The QNMs obtained appear in Table II and Table III, showing real and imaginary parts of ω, with mass re-scaled back to $M = 1$ for easier comparison with literature.

At the $\alpha = 0$ limit, one recovers purely gravitational QNMs for $V_{i=2}^{(-)}$ in Table III and purely electromagnetic QNMs for $V_{i=1}^{(-)}$ in Table II. It is worth mentioning that just like in GR, there is no gravitational radiation carried in dipolar perturbations. Because the gravitational charge of the vector field is $Q_g = \sqrt{\alpha G_N}M > 0$ and $M > 0$, Q_g is never negative making it impossible for MOG to have dipole radiation [22]. Lastly, we performed a complete scan of the space for all modes with $\ell = 1,2,3$ and $\ell = 2,3,4$ in both sectors Z_1 and Z_2 respectively, and no unstable QNMs with $\text{Im}(\omega) > 0$ were found.

Some comments on the higher $(n = 3)$ overtones are perhaps necessary. In general, to ensure accuracy of the results the AIM code was compiled successively for increasing number of iterations until no variation in the value of QNMs was observed. Usually, runs at 400 and 500 iterations yielded the same frequencies in every case, except for $n \gg \ell$ as in Table II for $\ell = 1$ and $n = 3$, where the frequencies stabilized at 600 and 700 iterations.

ℓ	n	$\alpha = 0$	$\alpha = 1$	$\alpha = 4$	$\alpha = 9$
1	0	0.2483 - 0.09249i	0.1448 - 0.04805i	0.06343 - 0.01881i	0.03268 - 0.009084i
	1	0.2145 - 0.2937i	0.1308 - 0.1506i	0.05882 - 0.05828i	0.03038 - 0.02796i
	2	0.1748 - 0.5252i	0.1135 - 0.2654i	0.05258 - 0.1014i	0.02675 - 0.04833i
	3	0.1462 - 0.7719i	0.1090 - 0.3866i	0.05036 - 0.1494i	0.02434 - 0.07008i
2	0	0.4576 - 0.09500i	0.2651 - 0.04917i	0.1164 - 0.01930i	0.06000 - 0.009351i
	1	0.4365 - 0.2907i	0.2565 - 0.1498i	0.1136 - 0.05854i	0.05861 - 0.02830i
	2	0.4012 - 0.5016i	0.2420 - 0.2563i	0.1087 - 0.09948i	0.05607 - 0.04791i
	3	0.3626 - 0.7302i	0.2257 - 0.3699i	0.1028 - 0.1425i	0.05272 - 0.06840i
3	0	0.6569 - 0.09562i	0.3771 - 0.04933i	0.1648 - 0.01936i	0.08493 - 0.009395i
	1	0.6417 - 0.2897i	0.3709 - 0.1492i	0.1627 - 0.05842i	0.08391 - 0.02831i
	2	0.6138 - 0.4921i	0.3594 - 0.2522i	0.1589 - 0.09841i	0.08198 - 0.04760i
	3	0.5779 - 0.7063i	0.3446 - 0.3600i	0.1537 - 0.1398i	0.07927 - 0.06743i

TABLE II. QNMs accurate to 4 decimal places for $M = 1$ scaled MOG electromagnetic perturbations $V_{i=1}^{(-)}$ for $\ell = 1$, $\ell = 2$ and $\ell = 3$ modes.

ℓ	n	$\alpha = 0$	$\alpha = 1$	$\alpha = 4$	$\alpha = 9$
2	0	0.3737 - 0.0890i	0.2220 - 0.04650i	0.1021 - 0.01867i	0.05431 - 0.009171i
	1	0.3467 - 0.2739i	0.2115 - 0.1423i	0.09872 - 0.05678i	0.05270 - 0.02781i
	2	0.3011 - 0.4783i	0.1937 - 0.2457i	0.09283 - 0.09696i	0.04974 - 0.04725i
	3	0.2515 - 0.7051i	0.1742 - 0.3579i	0.08582 - 0.1397i	0.04584 - 0.06776i
3	0	0.5994 - 0.0927i	0.3353 - 0.04758i	0.1496 - 0.0189i	0.07875 - 0.009267i
	1	0.5826 - 0.2813i	0.3281 - 0.1441i	0.1472 - 0.0571i	0.07761 - 0.02795i
	2	0.5517 - 0.4791i	0.3149 - 0.2444i	0.1428 - 0.0964i	0.07543 - 0.04706i
	3	0.5120 - 0.6903i	0.2979 - 0.3503i	0.1368 - 0.1373i	0.07238 - 0.06680i
4	0	0.8092 - 0.0942i	0.4452 - 0.04804i	0.1965 - 0.01903i	0.1030 - 0.009311i
	1	0.7966 - 0.2843i	0.4398 - 0.1449i	0.1947 - 0.05731i	0.1021 - 0.02802i
	2	0.7727 - 0.4799i	0.4294 - 0.2441i	0.1912 - 0.09625i	0.1004 - 0.04699i
	3	0.7398 - 0.6839i	0.4151 - 0.3468i	0.1863 - 0.1362i	0.09796 - 0.06636i

TABLE III. QNMs accurate to 4 decimal places for $M = 1$ scaled MOG gravitational perturbations $V_{i=2}^{(-)}$ for $\ell = 2$, $\ell = 3$ and $\ell = 4$ modes.

In Table II and Table III, the QNMs are displayed for a scaled mass $M = 1$ in order to illustrate the difference in magnitude with the result of general relativity. However, if we impose the same scaling condition $G_N M = 1$ from GR to MOG we obtain $GM = G_N(1 + \alpha)M = 1$ thus yielding $M = \frac{1}{1+\alpha}$. Consequently, we can observe that the QNMs will be increased by a factor of $(1 + \alpha)$ and these will correspond to lower mass black holes than those predicted by GR. Table IV and Table V show this.

By inspection of Table IV and Table V, we can see that the damping given by $\text{Im}(\omega)$ of the QNMs for $\alpha = 1$, $\alpha = 4$ and $\alpha = 9$ (corresponding to black holes that are $1/2$, $1/5$ and $1/10$ as massive, respectively, compared to its $\alpha = 0$ counterpart) matches almost identically the damping predicted by GR. On the other hand, for increasing model parameter α, the actual frequency of the QNM given by $\text{Re}(\omega)$ deviates and is significantly greater than that of GR. This provides another key experimental signature of MOG in the ringdown phase.

ℓ	n	$\alpha = 0$	$\alpha = 1$	$\alpha = 4$	$\alpha = 9$
1	0	0.2483 - 0.09249i	0.2896 - 0.09611i	0.3171 - 0.09403i	0.3268 - 0.09084i
	1	0.2145 - 0.2937i	0.2616 - 0.3012i	0.2941 - 0.2914i	0.3038 - 0.2796i
	2	0.1748 - 0.5252i	0.2271 - 0.5309i	0.2629 - 0.5072i	0.2675 - 0.4833i
	3	0.1462 - 0.7719i	0.2179 - 0.7733i	0.2518 - 0.7470i	0.2434 - 0.7008i
2	0	0.4576 - 0.09500i	0.5302 - 0.09833i	0.5821 - 0.09650i	0.6000 - 0.09351i
	1	0.4365 - 0.2907i	0.5131 - 0.2995i	0.5680 - 0.2927i	0.5861 - 0.2830i
	2	0.4012 - 0.5016i	0.4840 - 0.5126i	0.5435 - 0.4974i	0.5607 - 0.4791i
	3	0.3626 - 0.7302i	0.4514 - 0.7397i	0.5139 - 0.7125i	0.5272 - 0.6840i
3	0	0.6569 - 0.09562i	0.7542 - 0.09867i	0.8239 - 0.09681i	0.8493 - 0.09395i
	1	0.6417 - 0.2897i	0.7418 - 0.2983i	0.8136 - 0.2921i	0.8391 - 0.2831i
	2	0.6138 - 0.4921i	0.7189 - 0.5045i	0.7944 - 0.4921i	0.8198 - 0.4760i
	3	0.5779 - 0.7063i	0.6891 - 0.7200i	0.7687 - 0.6988i	0.7927 - 0.6743i

TABLE IV. QNMs accurate to 4 decimal places for $M = 1/(1 + \alpha)$ scaled MOG electromagnetic perturbations $V_{i=1}^{(-)}$ for $\ell = 1$, $\ell = 2$ and $\ell = 3$ modes.

ℓ	n	$\alpha = 0$	$\alpha = 1$	$\alpha = 4$	$\alpha = 9$
2	0	0.3737 - 0.0890i	0.4441 - 0.09300i	0.5105 - 0.09333i	0.5431 - 0.09171i
	1	0.3467 - 0.2739i	0.4229 - 0.2847i	0.4936 - 0.2839i	0.5270 - 0.2781i
	2	0.3011 - 0.4783i	0.3874 - 0.4914i	0.4642 - 0.4848i	0.4974 - 0.4725i
	3	0.2515 - 0.7051i	0.3484 - 0.7158i	0.4291 - 0.6985i	0.4584 - 0.6776i
3	0	0.5994 - 0.0927i	0.6706 - 0.09516i	0.7479 - 0.09456i	0.7875 - 0.09267i
	1	0.5826 - 0.2813i	0.6563 - 0.2882i	0.7360 - 0.2856i	0.7761 - 0.2795i
	2	0.5517 - 0.4791i	0.6298 - 0.4888i	0.7138 - 0.4821i	0.7543 - 0.4706i
	3	0.5120 - 0.6903i	0.5957 - 0.7006i	0.6842 - 0.6865i	0.7238 - 0.6680i
4	0	0.8092 - 0.0942i	0.8904 - 0.09608i	0.9826 - 0.09513i	1.030 - 0.09311i
	1	0.7966 - 0.2843i	0.8795 - 0.2898i	0.9735 - 0.2865i	1.021 - 0.2802i
	2	0.7727 - 0.4799i	0.8588 - 0.4881i	0.9560 - 0.4812i	1.004 - 0.4699i
	3	0.7398 - 0.6839i	0.8301 - 0.6936i	0.9315 - 0.6810i	0.9796 - 0.6636i

TABLE V. QNMs accurate to 4 decimal places for $M = 1/(1 + \alpha)$ scaled MOG gravitational perturbations $V_{i=2}^{(-)}$ for $\ell = 2$, $\ell = 3$ and $\ell = 4$ modes.

FUTURE DIRECTIONS

Attempts will be made in future work to calculate the MOG QNMs using the Kerr-MOG metric solution including the spin parameter a. It is anticipated that the spins of the merging black holes will play an important role when interpreting the aLIGO/Virgo ringdown data, given that after merger the resulting black hole has always showed spin greater than zero.

Other avenues to explore with QNMs include the study of gravitational wave echoes. With the discovery of gravitational waves from compact binary mergers came a more careful study of exotic compact objects (ECOs) as alternatives of black holes. Theoretically, the existence of horizonless ECOs may be fundamental to resolving the black hole information paradox. Empirically it is hard to verify the nature of spacetime very close to the horizon due to the large gravitational redshift, and observational evidence from astrophysical objects only shows that ECOs must resemble black holes considerably further from the horizon [44] [45]. Short wavelength modes, which can be approximated by point particles in comparison to the size of the object, have a tiny escape cone and are efficiently trapped in the high redshift region. Very compact ECOs will then appear dark in the electromagnetic window. Gravitational waves with wavelengths comparable to the size of the object may not suffer from the trapping.

As recently highlighted in [46] [47], the LIGO observation of the black hole merger and ringdown does not exclude horizonless ECOs that have the same light ring potential outside of the horizon. Rather, new observational signals may occur afterwards due to reflection from ECO surfaces or interiors situated well within the light ring. The reflected waves will impinge back on the potential barrier at the light ring after some time delay, with some transmitted to the outside and some reflected back in.

This process repeats and generates a distinct set of echoes as seen by an outside observer. The time delay t_d between two consecutive echoes is closely related to the compactness of the object. Interestingly it depends logarithmically on the distance from the would-be horizon to where deviations occur, and in this way it can probe Planck-scale physics.

An interesting question to pose would be if there are compact objects in MOG that can reproduce gravitational wave echoes. We already know that its horizon structure is different compared to its classical GR counterpart, so maybe this can translate into new interesting physics for gravitational waves near the horizon. Such studies are timely in light of the tentative detection of gravitational-wave echoes in the post-merger signal of GW170817 claimed at the 4.2σ significance level [48] [49].

CONCLUSION

We have investigated the quasinormal modes for gravitational and electromagnetic perturbations in the ringdown phase of the merging of two MOG black holes based on the STVG (MOG) theory. The black holes are MOG generalizations of the static, spherically symmetric Schwarzschild black hole in GR. For the parameter $\alpha > 0$ according to $G = G_N(1 + \alpha)$, there is a significant reduction in the frequencies for MOG gravitational perturbations for $\ell = 2, \ell = 3$ and $\ell = 4$ modes, and for $\ell = 1, \ell = 2, \ell = 3$ MOG electromagnetic perturbations. This will allow for a possible distinguishing signal between MOG and GR for sufficiently sensitive frequency determinations. The detection of ~ 50 gravitational wave events by the aLIGO/Virgo observatories can be expected to produce accurate enough frequency results during the waveform ringdown phase. Such number of detections is required to meet the criteria of a Signal to Noise Ratio (SNR) ~ 35 event of $30M_\odot$ - $30M_\odot$ POP III BH - BH mergers needed to detect the first few modes [43].

ACKNOWLEDGMENTS

REFERENCES

1. B. P. Abbott *et al.* [LIGO Scientific and Virgo Collaborations], Phys. Rev. Lett. **116**, 061102 (2016) [arXiv:1602.03837 [gr-qc]].
2. B. P. Abbott *et al.* [LIGO Scientific and Virgo Collaborations], Phys. Rev. Lett. **116**, no. 24, 241103 (2016) [arXiv:1606.04855 [gr-qc]].
3. B. P. Abbott *et al.* [LIGO Scientific and VIRGO Collaborations], Phys. Rev. Lett. **118**, no. 22, 221101 (2017) [arXiv:1706.01812 [gr-qc]].
4. B. P. Abbott *et al.* [LIGO Scientific and Virgo Collaborations], Astrophys. J. **851**, no. 2, L35 (2017) [arXiv:1711.05578 [astro-ph.HE]].
5. B. P. Abbott *et al.* [LIGO Scientific and Virgo Collaborations], Phys. Rev. Lett. **119** (2017) no.14, 141101
6. B. P. Abbott *et al.* [LIGO Scientific and Virgo Collaborations], Phys. Rev. Lett. **119**, no. 16, 161101 (2017)
7. B. P. Abbott *et al.* [LIGO Scientific and Virgo Collaborations], Phys. Rev. Lett. **116**, no. 22, 221101 (2016) [arXiv:1602.03841 [gr-qc]].
8. R. A. Konoplya and A. Zhidenko, Rev. Mod. Phys. **83**, 793 (2011) [arXiv:1102.4014 [gr-qc]].
9. D. B. Sibandze, R. Goswami, S. D. Maharaj and P. K. S. Dunsby, "Echoes from the black holes: Evidence of higher order corrections to General Relativity in strong gravity regime," arXiv:1702.04926 [gr-qc].
10. P. D. Lasky and D. D. Doneva, Phys. Rev. **D82**, 124068 (2010) [arXiv:1011.0747 [gr-qc]].
11. S. Bhattacharyya and S. Shankaranarayanan, "Quasinormal modes as a distinguisher between general relativity and f(R) gravity," arXiv:1704.07044 [gr-qc].
12. K. D. Kokkotas and B. G. Schmidt, Living Rev. Rel. **2**, 2 (1999) [gr-qc/9909058].
13. V. Cardoso, E. Franzin and P. Pani, Phys. Rev. Lett. **116**, no. 17, 171101 (2016) Erratum: [Phys. Rev. Lett. **117**, no. 8, 089902 (2016)] [arXiv:1602.07309 [gr-qc]].
14. L. M. Goggin, "A Search For Gravitational Waves from Perturbed Black Hole Ringdowns in LIGO Data," arXiv:0908.2085 [gr-qc].
15. B. P. Abbott *et al.* [LIGO Scientific Collaboration], Phys. Rev. **D80**, 062001 (2009) [arXiv:0905.1654 [gr-qc]].
16. J. Aasi *et al.* [LIGO Scientific and VIRGO Collaborations], Phys. Rev. **D89**, no. 10, 102006 (2014) [arXiv:1403.5306 [gr-qc]].
17. E. Berti, V. Cardoso and C. M. Will, Phys. Rev. **D73**, 064030 (2006) [gr-qc/0512160].
18. L. London, D. Shoemaker and J. Healy, Phys. Rev. **D90**, no. 12, 124032 (2014) Erratum: [Phys. Rev. **D94**, no. 6, 069902 (2016)][arXiv:1404.3197 [gr-qc]].

19. K. Sakai, K. I. Oohara, H. Nakano, M. Kaneyama and H. Takahashi, "Estimation of starting times of quasi-normal modes in ringdown gravitational waves with the Hilbert-Huang transform," arXiv:1705.04107 [gr-qc].
20. H. T. Cho, A. S. Cornell, J. Doukas, T. R. Huang and W. Naylor, Adv. Math. Phys. **2012**, 281705 (2012)
21. J. W. Moffat, JCAP 0603, 004 (2006). [arXiv:gr-qc/0506021].
22. J. W. Moffat, Phys. Lett. **B763**, 427 (2016), [arXiv:1603.05225 [gr-qc]].
23. J. W. Moffat, Eur. Phys. J. C**75**, 175 (2015), [arXiv:1412.5429 [gr-qc]].
24. J. W. Moffat, Eur. Phys. J. C **75**, 130 (2015), [arXiv:1502.01677 [gr-qc]].
25. J. W. Moffat, "Misaligned Spin Merging Black Holes in Modified Gravity (MOG)", arXiv:1706.05035 [gr-qc].
26. J. W. Moffat and S. Rahvar, MNRAS **436**, 1439 (2013), [arXiv:1306.6383 [astro-ph.GA]].
27. J. W. Moffat and S. Rahvar, MNRAS **441**, 3724 (2014), [arXiv:1309.5077 [astro-ph.CO]].
28. J. W. Moffat and V. T. Toth, Phys. Rev. **D91**, 043004 (2015), [arXiv:1411.6701 [astro-ph.GA]].
29. J. W. Moffat, arXiv:1510.07037 [astro-ph.CO].
30. J. W. Moffat, arXiv:1410.2464 [gr-qc].
31. F. Shojai, S. Cheraghchi and H. Bouzari Nezhad, Phys. Lett. **B 770**, 43 (2017), [arXiv:1704.04161 [gr-qc]].
32. V. Ferrari and B. Mashhoon, Phys. Rev. **D30**, 295-304 (1984).
33. E. W. Leaver, Proc. Roy. Soc. Lond. **A402**, 285-298 (1985).
34. B. Mashhoon, Proceedings of the Third Marcel Grossmann Meeting on Recent Developments of General Relativity, edited by H. Ning, p. 599, Amsterdam, 1983, North-Holland; B. F. Schutz and C. M. Will, Astrophys. J. L291, 33 (1985); E. Seidel, S. Iyer, Phys. Rev. **D41**, 374-382 (1990).
35. T. Barakat, Int. J. Mod. Phys. **A21**, 4127-4135 (2006).
36. H. Ciftci, R. L. Hall, N. Saad, J. Phys. **A36**, 11807-11816 (2003); Phys. Lett. A340, 388-396 (2005).
37. H. Ciftci, R. L. Hall, N. Saad, J. Phys. **A36**, 11807-11816 (2003); Phys. Lett. A340, 388-396 (2005).
38. H. T. Cho, A. S. Cornell, J. Doukas, W. Naylor, Class. Quant. Grav. **27**, 155004 (2010). [arXiv:0912.2740 [gr-qc]].
39. F. J. Zerilli, Phys. Rev. **D9**, 860-868 (1974).
40. V. Moncrief, Phys. Rev. **D9**, 2707-2709 (1974).
41. V. Moncrief, Phys. Rev. **D12**, 1526-1537 (1975).
42. E. W. Leaver, Phys. Rev. **D41**, 2986-2997 (1990).
43. T. Nakamura, H. Nakano and T. Tanaka, Phys. Rev. D **93**, no. 4, 044048 (2016)
44. M. A. Abramowicz, W. Kluzniak and J. P. Lasota, Astron. Astrophys. **396**, L31 (2002)
45. V. Cardoso and P. Pani, arXiv:1707.03021 [gr-qc].
46. B. Guo, S. Hampton and S. D. Mathur, arXiv:1711.01617 [hep-th].
47. V. Cardoso, E. Franzin and P. Pani, Phys. Rev. Lett. **116**, no. 17, 171101 (2016)
48. J. Abedi, H. Dykaar and N. Afshordi, Phys. Rev. D **96**, no. 8, 082004 (2017)
49. J. Abedi and N. Afshordi, arXiv:1803.10454 [gr-qc].